

Formation of Fatigue Cracks in Copper Film Electroplated on Plastics

プラスチックに電着した銅薄膜における疲れき裂形成

by Yoshiaki HAGIUDA* and Masahisa MATSUNAGA*

萩生田 善明・松永 正久

1. Introduction

Although initial cracks are hardly observable on wrought metals in fatigue test, they are easily observed on thin electrodeposit, and they are uniformly distributed on the surface¹⁾ as shown in Fig.1; because of smoothness of the surface with neither defect nor pit, and of uniformity of stress distribution. Since the number of initiated cracks can be counted and their growing length can also be measured in the course of the fatigue tests, observation of these cracks may produce valuable information to the theory of crack formation.

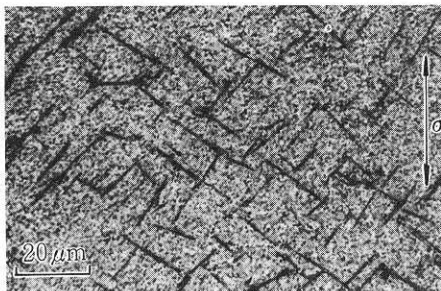


Fig. 1 An example of uniformly distributed cracks for repeated bending test.

These uniformly distributed cracks do not appear in every condition. In this report, crack modes in various conditions will be described.

2. Formation of Uniformly Distributed Cracks

In repeated bending test of the previous report¹⁾, it was found that the uniformly distributed cracks appeared when the strain amplitude was 1.2 to 1.7 × 10⁻³, that is, 7 to 9 kg/mm² of stress amplitude for copper film, and thickness of the electrodeposition was about 30 μm. In these testing conditions, the initiation of cracks and their growth could be observed. Direction of these cracks would corre-

sponds to that of the maximum shearing stress. A histogram of the direction of the cracks are shown in Fig. 2.

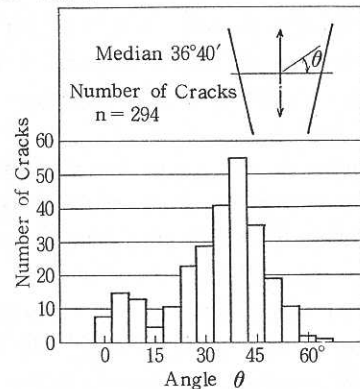


Fig. 2 Angular distribution for uniformly distributed cracks by repeated bending test.

The angle θ of 294 cracks longer than 5 μm were measured, which located on a line apart from the fixed point by 25 mm. The figure shows a small deviation from the direction of the maximum shearing stress, $\theta = 45^\circ$. Causes of the deviation was not clarified. In repeated pure bending test and in repeated torsion test, the direction of the most of cracks were along the direction of the maximum shearing stress¹⁾. Fig. 3. shows the uniformly distributed cracks and their connection in repeated pure bending test, and shows that the cracks orientate along

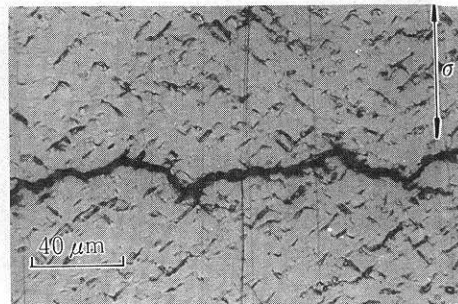


Fig. 3 Uniformly distributed cracks for repeated pure bending test

*Dept. of Mechanical Engineering and Naval Architecture, Institute of Industrial Science, Univ. of Tokyo.

研究速报
 the direction of the maximum shearing stress.

3. Effect of Stress and Film Thickness

In smaller stress range in which the strain amplitude was under 1.0×10^{-3} , that is, the stress amplitude of copper was 4.7 to 5.2 kg/mm², the uniformly distributed cracks appeared in a small number and they were connected or initiated into a main crack. However, the elongation in tensile test of copper film which was dissolved from ABS plastics, was reduced to a value of 30 to 90 per cent compared with that of original deposits. In larger stress range, a main crack grew from the edge of the specimen.

An experiment on the effect of film thickness was performed by torsion test, in which the stress amplitude $\gamma = 1.03 \times 10^{-3}$ and 1.4×10^{-3} were chosen and thickness was under 20 μm and over 40 μm . In a specimen with film thickness of under 20 μm , the fracture occurred after $N = 5 \times 10^5$ and 7×10^5 at $\gamma = 1.4 \times 10^{-3}$ and $\gamma = 1.03 \times 10^{-3}$, respectively. The fracture took place from a defect and crossed to the axis at 45°. The distributed cracks co-existed in both cases. The cracks grew from a pit on the deposit.

The length of uniformly distributed cracks increased and their number decreased as the thickness of the deposit increased. In a specimen of 60 μm thickness, a stage II crack propagated from one of the distributed cracks. The stage II crack in this experiment was that of shear type as shown in Fig. 4, which shows a crack on a specimen of 60 μm thick. The specimen was ruptured after $N = 8.78 \times$

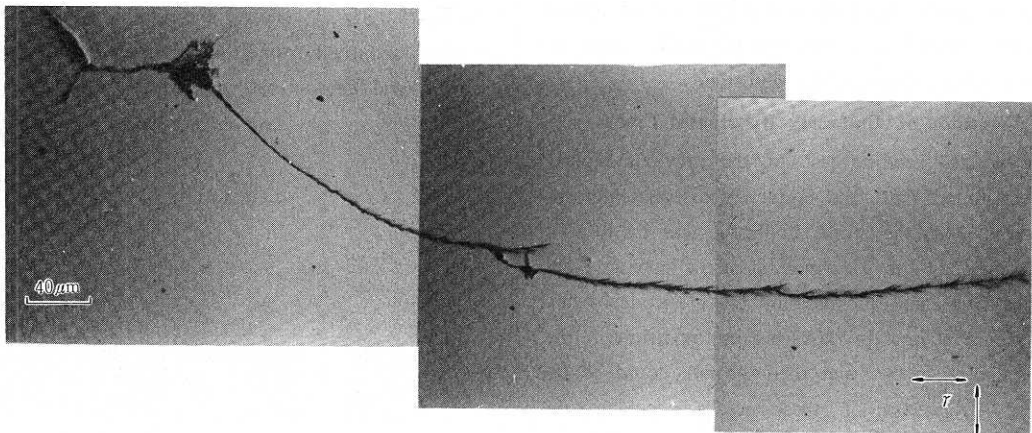


Fig. 4 Stage II cracks of shear type which propagated from one of the uniformly distributed cracks $\gamma = 1.03 \times 10^{-3}$, $N = 8.78 \times 10^5$, $t = 60 \mu\text{m}$

10^5 in $\gamma = 1.03 \times 10^{-3}$. Nearly the same mode of crack was observed on a specimen with a pit of 0.3 mm diameter, from which cracks grew. This stage II cracks were accompanied sometimes by vertical cracks and/or branched cracks as shown in Fig. 5.

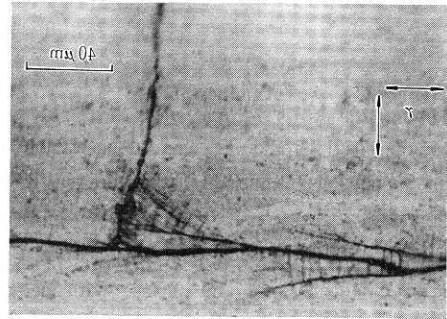


Fig. 5 Stage II cracks of shear type accompanied by branches

4. Effect of Grain Size

Effect of grain size was examined on specimens electrodeposited from several kinds of solutions and annealed specimens as shown in Table 1. Nearly the

Table 1. Electrodeposits with various grain size

Name	Method of Preparation	Grain Diameter (μm)
A	Electrodeposited from sulfate solution with brightner A	0.2~0.3
B	Electrodeposited from sulfate solution with brightner B	about 1
C	Electrodeposited from strike copper solution	1 ~ 2
D	Annealed at 370°C in vacuum	about 5
E	Electrodeposited single crystal	-

same results were obtained with specimen A and B in which the uniformly distributed cracks were linear, along a direction of the maximum shearing force and penetrated the grains. In specimens C and D, the uniformly distributed cracks occurred along the direction of the maximum shearing stress which coincided with the direction of slip plane of each crystal. These cracks are shown in Fig. 6. Fig. 7 shows an electronmicrograph of the cracks on specimen C.

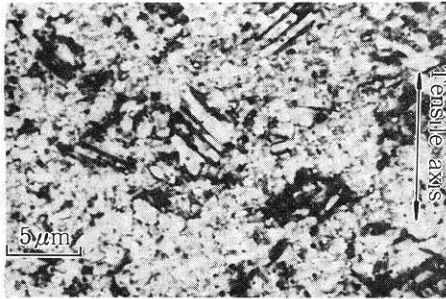


Fig. 6 Uniformly distributed cracks on deposit with larger grain size



Fig. 7 Electronmicrograph of the cracks on copper strike surface

5. Conclusion

It was discovered by these experiments that the uniformly distributed cracks growing along the direction of the maximum shearing stress had their limitation in the maximum length depending on their film thickness. The phenomenon was explained by the authors as follows: The uniformly distributed cracks are originated from a slip in a crystal on the surface, propagated along slip planes or along grain boundaries to the direction of the maximum shearing stress, linearly on the surface and circularly to the interface. When the leading head arrives at the interface, a crack of nearly the same size is formed at the surface as shown in Fig. 9. In order that

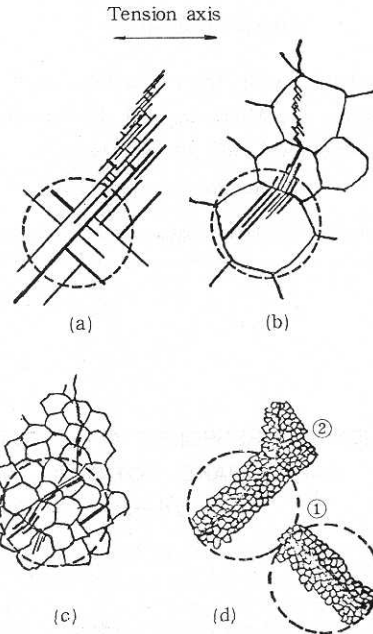


Fig. 8 Transition of stage I crack to stage II crack. Different mode for different grain size. Dotted circles indicate the hypothesized ranges in which the shearing stress is effective (a) single crystal (b) annealed copper (c) copper strike (d) minute grain size

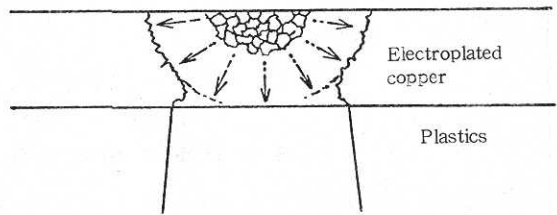


Fig. 9 Schematic drawing for formation of uniformly distributed cracks

the cracks extend beyond this range, a stage II crack must grow along the direction perpendicular to the tension axis, as shown in Fig. 8.

The growth rate of the uniformly distributed cracks was much slower than that of the stage II cracks and was of the same order of the cracks on single crystal copper by McEvily and Boettner.²⁾ The present authors also obtained the same result with single crystal films. They concluded that these cracks were classified into stage I cracks in observing the growth rate. They also found that there exist the stage II cracks which propagate to a direction of maximum shearing stress.

Acknowledgement

The authors would like to express their thanks to Professors H. Miyamoto and H. Kitagawa for their encouragement and kind discussions.

(Manuscript received, March 11, 1977)

References

- 1) M. Matsunaga and Y. Hagiuda, Proc. 8th INTERNATIONAL FINISH, Forster-Verlag AG., 1973 p. 377
- 2) A. J. McEvily Jr. and R. C. Boettner, Acta Metall., 11, 725, 1963

東京大学生産技術研究所報告 刊行

第26巻 第6号 (英文)

佐藤 壽 芳著

A STUDY ON RESPONSE CHARACTERISTIC OF BUILDING-APPENDAGE STRUCTURE FOR EARTHQUAKE MOTIONS WITH TWO GROUND PREDOMINANT PERIODS

卓越周期成分が二つの地震動にたいする構築物・機器系の応答特性に関する研究

構造物の耐震設計に用いられる震度の決定には応答曲線が参考とされる。本報告は、二つの地盤卓越周期を仮定し、不規則振動論により模擬された地震動から求められる応答曲線によって、地震動について求められている応答曲線の性質を明らかにし、より合理的な耐震設計を可能ならしめることを目的としたものである。

本報告に関連するこれまでの研究と本研究の必要性について1章でのべている。2章では、これまでの大地震記録にたいする応答曲線の解析から、応答曲線の最大倍率値が大地震時の記録にたいするもの程大きくなっており、模擬地震動によるこれまでの応答曲線解析の経緯を考慮して、二つ以上の地盤卓越周期を仮定する必然性を明らかにしている。3章では、構築物を考えた1自由度系、この上の上の付加機器系を考えた2自由度系に関して、二つの地盤卓越周期を想定した模擬地震動を用いることにより、地震動について求められている応答曲線の性質を、定量的、定性的によく説明しうることを明らかにしている。4章では、3章で扱った系で、構築物系に完全弾塑性特性を考え、等価線型系とした解析により模擬地震動にたいする応答曲線を求め、やはり地震動について求められている応答曲線の性質を説明しうることを示している。5章では、地盤卓越周期、構築物固有期、減衰定数等系のパラメータが設計値にたいして本来統計的性質を有するものとの観点から、応答曲線の平均値、分散を推定している。6章は以上の研究に関する結論である。

(1977年3月発行)

第26巻 第7号 (和文)

曾我部 潔・重田 達也・柴田 碧著

液体貯槽の耐震設計に関する基礎的研究

著者らはここ数年間液体貯槽の耐震設計について研究を行ってきた。本報告はこの間に行なった一連の実験および解析によって得られた経験をもとにして、液体貯槽の耐震設計に対する一つの体系化を行なおうとしたものである。

まず最初に、液体貯槽とスロッシング(液面動揺)現象、液体貯槽の耐震設計の現状および問題点、液体貯槽の各種地震被害および地震によるタンク破損のメカニズムについて示し、これをもとにして液体貯槽の耐震設計の体系化を行なうための基本概念について示している。

次に、この基本概念にもとづき、軸対称液体貯槽のスロッシングの固有値解析、大型円筒貯槽模型の自然地震応答観測実験、円筒タンクの応答解析、地震時における円筒タンクの横ずれ現象の解析および球形タンクの応答解析などを行なっている。

本報告では、これら一連の実験・解析で得られた結果を実際の設計に便利な図表等に整理している。

上述の各項目について、いまいし詳しく説明すると次のとおりである。

軸対称液体貯槽のスロッシングの固有値解析では、一般の軸対称容器内部の液体のスロッシングの固有周期等を計算するための簡単な手法の提案を行なっている。

大型円筒貯槽模型の自然地震応答観測実験では、大型の液体貯槽模型(直径4m, 高さ2m)をコンクリートの基礎の上に設置し、自然地震時における液面変位、側面圧力および容器のひずみの観測を行なった結果について示している。

円筒タンクの応答解析では、まず円筒タンクが地震動を受けた場合のスロッシングの応答解析のための基礎式の誘導を行なっている。次に、この結果と上述の自然地震応答観測の結果とを考え合わせて、地震時におけるスロッシングの応答を、正弦波入力に対する過渡応答で推定するスロッシングの応答の簡易計算法の提案を行なっている。

地震時における円筒タンクの横ずれ現象の解析では、まず小型の円筒タンク模型(直径40cm)を水平振動と上下振動を同時に受ける振動台上に加振する実験を行ない、横ずれ現象の発生領域を求めている。次に上述の円筒タンクの応答解析の手法を用いて、円筒タンクの横ずれ現象の発生領域を求め、実験結果と比較・検討している。

球形タンクの応答解析では、まず小型の球形容器模型(直径50cm)を振動台上に固定し、正弦波共振実験により球形タンクの基本振動特性の解明を行なっている。次にこの結果をもとにして、球形タンクが地震波の入力を受けた場合の応答を計算する方法について示している。

(1977年3月発行)